

# Investigating the Cherenkov light production due to cross-talk in closely stored nuclear fuel assemblies in wet storage

Erik Branger, Sophie Grape, Peter Jansson, Erik Andersson Sundén, Staffan Jacobsson Svärd

Uppsala University, Uppsala, Sweden

E-mail: erik.branger@physics.uu.se

## Abstract:

The Digital Cherenkov Viewing Device (DCVD) is one of the tools available to a safeguards inspector performing verifications of irradiated nuclear fuel assemblies in wet storage. One of the main advantages of safeguards verification using Cherenkov light is that it can be performed without moving the fuel assemblies to an isolated measurement position, allowing for quick measurements. One disadvantage of this procedure is that irradiated nuclear fuel assemblies are often stored close to each other, and consequently gamma radiation from one assembly can enter a neighbouring assembly, and produce Cherenkov light in the neighbour. As a result, the measured Cherenkov light intensity of one assembly will include contributions from its neighbours, which may affect the safeguards conclusions drawn.

In this paper, this so-called near-neighbour effect, is investigated and quantified through simulation. The simulations show that for two fuel assemblies with similar properties stored closely, the near-neighbour effect can cause a Cherenkov light intensity increase of up to 3% in a measurement. For one fuel assembly surrounded by identical neighbour assemblies, a total of up to 14% of the measured intensity may emanate from the neighbours. The relative contribution from the near-neighbour effect also depends on the fuel properties; for a long-cooled, low-burnup assembly, with low gamma and Cherenkov light emission, surrounded by short-cooled, high-burnup assemblies with high emission, the measured Cherenkov light intensity may be dominated by the contributions from its neighbours.

When the DCVD is used for partial-defect verification, a 50% defect must be confidently detected. Previous studies have shown that a 50% defect will reduce the measured Cherenkov light intensity by 30% or more, and thus a threshold has been defined, where a  $\geq 30\%$  decrease in Cherenkov light indicates a partial defect. However, this work shows that the near-neighbour effect may also influence the measured intensity, calling either for a lowering of this threshold or for the intensity contributions from neighbouring assemblies to be corrected for. In this work, a method is proposed for assessing the near-neighbour effect based on declared fuel parameters, enabling the latter type of corrections.

**Keywords:** DCVD; partial defect verification; Cherenkov light; Geant4; Cross-talk

## 1. Introduction

Irradiated nuclear fuel assemblies are commonly stored in water for radiation protection, as well as for decay heat removal. As a result of the interactions of the radiation emanating from the fuel assemblies with the surrounding water, Cherenkov light is produced. This Cherenkov light has frequently been assessed by safeguards inspectors, using the presence, characteristics and intensity of the Cherenkov light to verify that the object under study is an irradiated nuclear fuel assembly, and not some other non-radioactive item.

The dominant path of Cherenkov light production is that gamma rays emitted in the decay of fission products enter the water, and are either photo-electrically absorbed or Compton-scatter off an electron. If the electron receives sufficient energy from the gamma ray, it will radiate Cherenkov light. In addition, high-energy beta-decay electrons can pass through the cladding and enter the water to produce Cherenkov light directly, though this contribution will be minor compared to the Cherenkov light produced by gamma decays. Neutrons cannot directly produce Cherenkov light since they have no electric charge, but radiation following a neutron interaction, such as e.g. inelastic scattering or fission of a uranium nuclei, can contribute. However, due to the low intensity of neutron emissions compared to gamma emissions, this contribution is expected to be negligible.

The Digital Cherenkov Viewing Device (DCVD) is one of the tools available to safeguards inspectors to measure the Cherenkov light emissions from irradiated nuclear fuel assemblies in wet storage. The DCVD can be used for gross-as well as partial-defect verification [1]. The type of partial defect analysis under study in this paper relies on comparisons of the measured intensities to predicted intensities, where removal or replacement of a fraction of the fuel rods will result in a lowered Cherenkov light intensity.

One of the main advantages of the DCVD is that the fuel assemblies do not have to be moved to an isolated area for measurement. A downside of measuring the assemblies where they are stored is that gamma radiation from closely stored assemblies can enter neighbouring

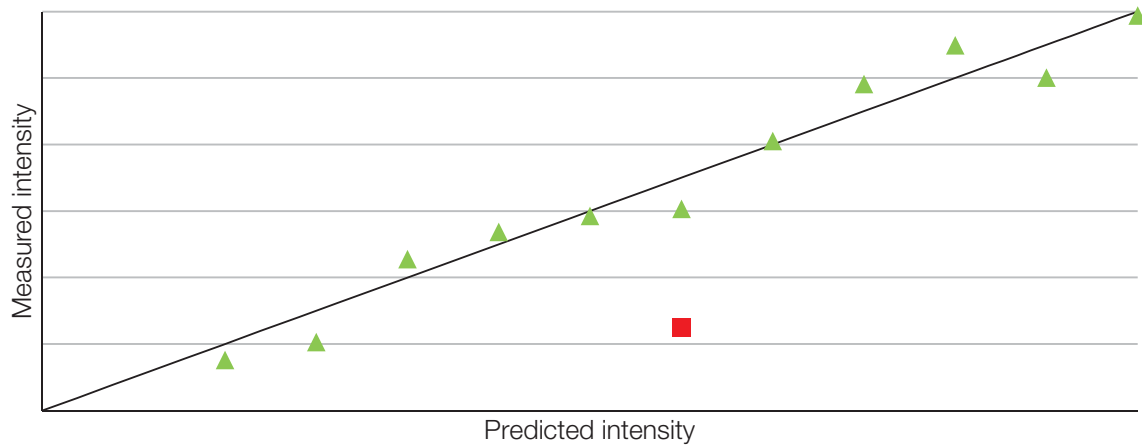


**Figure 1:** Illustration of the calibration procedure and partial defect verification method using the DCVD. For each fuel type, a linear fit is made between the predicted and measured intensity, where the fitted slope relates the predicted and measured intensity values. If any measured value deviates by more than 30% from the predicted (red square), a partial defect may be suspected.

assemblies and cause Cherenkov light emission there. This cross-talk, referred to as the near-neighbour effect, introduces a measurement error that is not compensated for in the currently deployed inspection procedure. The aims of this paper are: (i) to characterize and quantify the near-neighbour effect under selected fuel storage conditions, (ii) to identify how the near-neighbour effect affects the partial-defect verification procedure currently used, and (iii) suggest a method for its compensation.

### 1.1 Partial defect verification of used nuclear fuel using the DCVD

There are two methods used to detect partial defects in nuclear fuel assemblies with the DCVD. The first method uses image analysis to detect empty rod positions, and can be used to detect any removed rods in visible positions, as seen from the measurement position above the fuel. The second method is used to detect possible substitution of 50% of the fuel rods in an assembly. This method relies on the comparison of the measured intensity to a predicted intensity, based on operator-provided fuel declarations. In this analysis, the measured fuel assemblies are grouped by fuel type, so that each group contains fuels with the same physical design. For calibration within each group, the measured and predicted intensities are related by a linear fitting, as illustrated in Figure 1. As a result of this calibration, the predicted intensity values do not correspond to absolute measured intensity, but to a relative intensity of all fuel assemblies of the same type, and deviations from the group's linear fit call for further investigations of possible reasons. It is known from simulations that if 50% of the rods in an assembly are substituted with non-radioactive rods, the Cherenkov light intensity will be reduced by at least 30% [2]. Thus, if any measured intensity of an assembly is more than 30% lower than expected, a partial defect may be suspected.

Up until recently, the prediction method used was based on a parameterization of the Cherenkov light intensity as

a function of burnup and cooling time in a BWR 8x8 configuration [3]. This method is currently being replaced by a new method [4], which more accurately considers the fuel irradiation history by calculating the inventory of fission products using ORIGEN [5], by considering the geometry of the fuel assemblies, and by including Cherenkov light intensity contributions from both gamma and beta decays [6].

### 1.2 DCVD measurements and the near-neighbour effect

During a measurement, the DCVD is typically mounted on the railing of a moveable bridge, looking down on the fuel storage pond. The fuel assemblies are typically stored densely enough that radiation from one fuel assembly may enter neighbouring assemblies and create Cherenkov light there. Due to the relatively long distance that the radiation must travel to reach a neighbour, only gamma-ray emissions are expected to contribute to the near-neighbour effect. The intensity of neutron emissions is too low in comparison to gamma emissions to contribute significantly, and the ranges of alpha and beta particles are too short to contribute. This work hence considers only Cherenkov light produced due to gamma-decays of fission products. The magnitude of the near-neighbour effect is a function of the distance between the fuels, the amount of storage rack material present in between the assemblies and the energy spectrum of the gamma-ray emissions, which depend on the fuel cooling time.

In Figure 2, an example is shown of the storage situation at the Swedish Central Interim Storage Facility for Spent Nuclear fuel (Clab), where 25 BWR fuels are stored in one fuel basket. The fuels are stored very close to each other, being separated by 4 mm of borated steel. At a reactor fuel pond, there is typically more distance in between the fuels for criticality safety reasons, and it is also more likely that fresh or low-burnup fuel is stored close to high-burnup fuel, which in turn may cause a significant near-neighbour

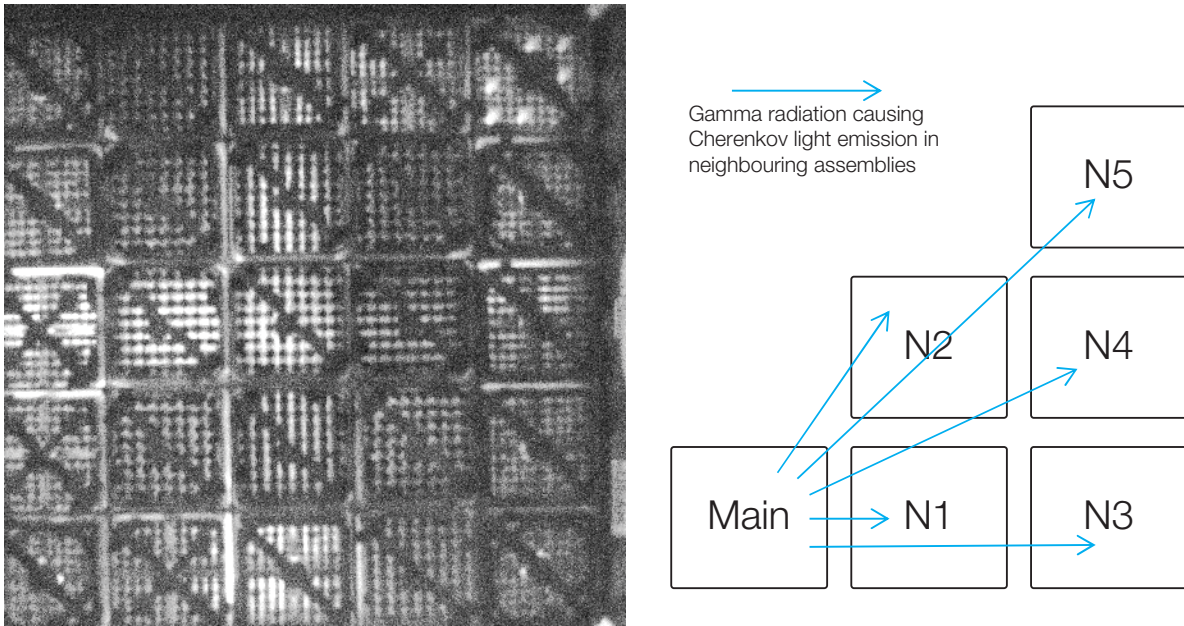


**Figure 2** : **Left**: DCVD image of 25 BWR fuels stored at the Swedish Central Interim Storage Facility for Spent Nuclear Fuel (Clab). Image courtesy of Dennis Parcey, Clab, and the Canadian Nuclear Safety Commission (CNSC). **Right**: For an active assembly emitting gamma radiation, called main, this paper analyses the Cherenkov light produced in the neighbouring assemblies, labelled N1 to N5, by gamma radiation originating from the main assembly. For symmetry reasons, all surrounding assemblies in a 5x5 grid may be defined using labels N1 to N5.

intensity in the low-burnup neighbours. Low-burnup fuel will give rise to relatively low levels of gamma emission and consequently low levels of Cherenkov light, in comparison to high-burnup, short-cooled fuel. Accordingly, a large fraction of the gamma radiation in a low burnup fuel may have its origin in neighbouring high-burnup fuel, thus a significant fraction of the Cherenkov-light emission in the low-burnup fuel may be attributed to the near-neighbour effect. To be able to refer to the different neighbouring position in a storage rack, Figure 2 also labels the five neighbour positions considered in this work, where position N1 shares one side with the main assembly causing the near-neighbour effect in the studies, N2 shares a corner with the main assembly, and N3-N5 are one row/column further away. Other positions in a 5x5 grid may be referred to using these labels due to the symmetry of the storage situation.

## 2. Definition and characterization of the near-neighbour effect

In this work, the near-neighbour effect is studied in terms of the effect of one assembly emitting gamma radiation (“Main” in Figure 2) to its neighbours (N1-N5). The results will be presented as the ratio, NNR, of the Cherenkov light intensity in a neighbour ( $I_{neighbour}$ ) produced by gamma radiation from the main assembly, as compared to the intensity in the main assembly itself ( $I_{main}$ ), or

$$NNR = \frac{I_{neighbour}}{I_{main}} \quad (1)$$

Note that by this definition, the intensity  $I_{main}$  is caused only by fission product decays in the main assembly. For real measurements, this value is not accessible due to the near-neighbour effect, though  $I_{main}$  can be predicted using one of the available prediction models [3] [6]. Furthermore, this study is limited to gamma-ray and bremsstrahlung emission, whereas it has been shown that beta particles may increase  $I_{main}$  by 1-10%, depending on fuel assembly type, irradiation history and cooling time [4]. There are negligible beta particle contributions to  $I_{neighbour}$  because of their short travel range in water.

### 2.1 Simulations

To characterize the near-neighbour effect, simulations were run for two different fuel assembly configurations, BWR 8x8 and PWR 17x17, and for two different fuel storage situations. The simulations were performed using a toolkit based on Geant4 [7], which is a further development of a previously used toolkit for simulating the Cherenkov light production in irradiated nuclear fuel [8].

The fuel assemblies were modelled including fuel rods and control-rod guide tubes for PWR, respectively a water channel and a fuel channel surrounding the rod configuration for BWR. The dimensions of the simulated fuel assemblies are given in Table 1. In addition, walls of a square steel storage rack were also included in the simulations. Vertically directed Cherenkov light was analysed in the simulations, since the DCVD will measure the vertical light component given the measurement situation with the DCVD situated above the fuel. Cherenkov light at an angle smaller than 3 degrees to the vertical axis was considered

representative of the vertical light component in the simulations, and this value also allows for comparisons with earlier simulation results [8]. This angle is wide enough that sufficient statistics can be obtained in the simulations in reasonable time, while being narrow enough to represent the vertical component.

	BWR 8x8	PWR 17x17
Number of fuel rods:	63	264
Fuel pellet diameter [mm]:	10.44	8.18
Cladding thickness [mm]:	0.91	0.57
Rod centre to centre distance [mm]:	16.3	12.6

**Table 1:** Dimensions of the simulated fuel assemblies.

The fuel depletion code ORIGEN [5] was used to assess the gamma spectrum for fuel assemblies with burnups of 10, 20, 30 and 40 MWd/kgU, and cooling times ranging from 0.25 to 60 years. The initial enrichment was set to 2% in all cases. These fuel parameter sets were chosen to be comparable to earlier studies [3] [8]. Fuels with 10, 20 and 30 MWd/kgU burnup were simulated as irradiated for four cycles, where each cycle consisted of 312.5 days of irradiation and 46 days of cooling, for a total of 1250 irradiation days. The power levels for the three lower burnups were 8, 16 and 24 kW/kgU, respectively. For the 40 MWd/kgU case, the power level remained at 24 kW/kgU, and the fuel was irradiated for 5 cycles. Note also that the gamma spectrum provided by ORIGEN includes both gamma-rays from fission product decays as well as bremsstrahlung produced when beta-particles are stopped in the fuel material.

**2.2 Effects of burnup and cooling time for BWR assemblies**

Figure 3 shows results of the simulations of the near-neighbour effect for BWR 8x8 fuels with a burnup of 40

MWd/kgU, for the fuel storage situation shown in Figure 2, with a 4 mm steel wall separating the assemblies. As can be seen, the N1 position is most strongly affected by the near-neighbour effect, with an NNR up to 2.9% of the main assembly intensity. For the N2 position, the near-neighbour effect is weaker, however; the NNR value is affected by attenuation in the assembly at N1, and will differ if the N1 position is occupied or vacant (called “N2” respectively “N2 only” in Figure 3). Accordingly, it is not only important to consider the properties of the emitting fuel assembly when estimating the near-neighbour effect; it is also important to consider which nearby positions that do not contain fuel to estimate the effect correctly. With N1 occupied, the intensity in N2 is up to 0.4% of the main assembly intensity, and with the N1 absent, it is up to 0.9%. For the N3 position, if N1 and N2 are occupied the near-neighbour effect is at most 0.05%, and could be neglected. However, if N1 and N2 are absent, the near-neighbour intensity in N3 can be up to 0.5% (called “N3 only” in Figure 3), comparable to the intensity found at N2. The intensities in the N4 and N5 positions were found to be negligible in all cases simulated.

As can also be seen in Figure 2, the near-neighbour intensity ratios NNR, (Eq. (1)), reach maxima at a cooling time of around 1 year. As an example, the N1 position has a maximum NNR value at 1 year of 2.9%, which decreases to 1.9% after 40 years cooling. This is due to the changing gamma spectrum of the fuel assembly with cooling time [9]. For short-cooled fuel, several high-energy gamma-emitting isotopes are still present, which have relatively long range and thus contribute more to the near-neighbour intensity. As the fuel cools, the gamma emissions become dominated by the 662 keV emissions of Cs-137, which are of lower energy and has a relatively shorter range. As a consequence of the changing gamma spectrum with time, compensating for the near-neighbour effect will require assessing the gamma spectrum of all assemblies

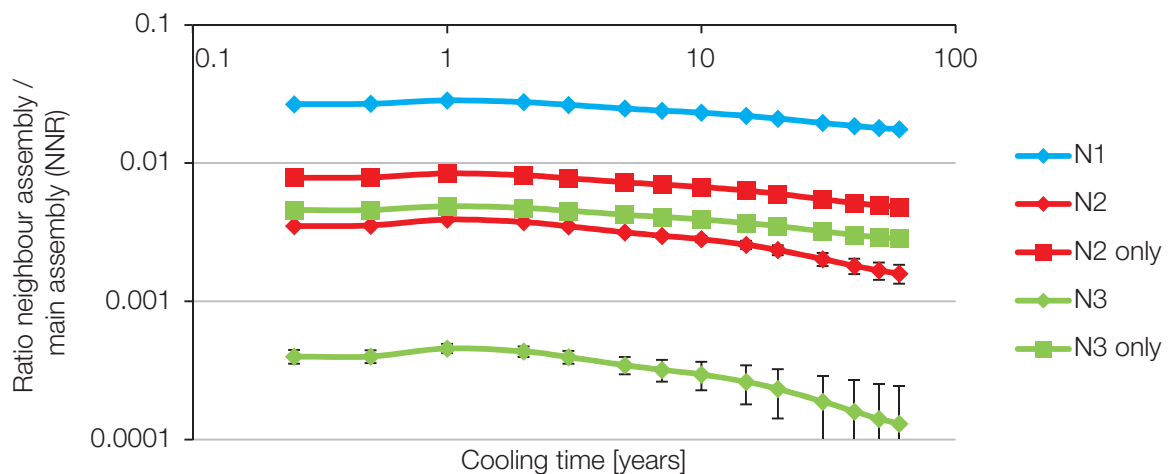


**Figure 3:** The magnitude of the near-neighbour effect as a function of cooling time, for BWR 8x8 assemblies. The N2 and N3 positions were simulated both for the situation that all neighbouring positions contained fuel (denoted N2 and N3, respectively), and for the situation that only two fuel assemblies were present, one at “main” and one at one neighbour position, (denoted “N2 only” and “N3 only”, respectively). Error bars denote 1  $\sigma$  uncertainty, and may be smaller than the point symbol for some data points.

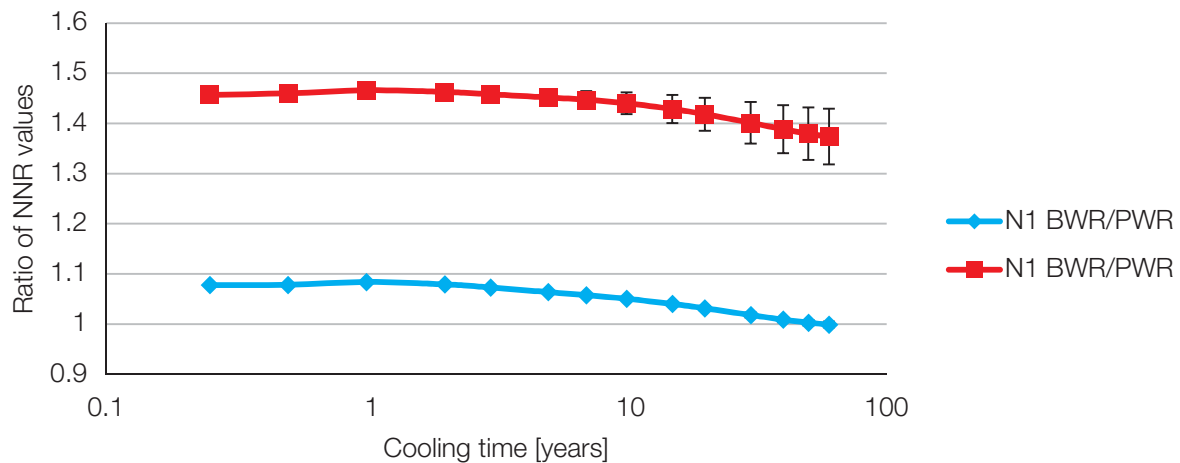


**Figure 4:** Ratio of NNR (see Eq. (1)) between BWR and PWR fuels as a function of cooling time, for the N1 and N2 neighbour storage positions. In the N2 case, all the N1 positions were occupied. Error bars denote  $1\sigma$  uncertainty, and may be smaller than the point symbol for some data points.

contributing to the measurable intensity at the event of measurement.

While the near-neighbour effect is noticeably affected by the cooling time, dependence on burnup is small, although a slight decrease with burnup is seen in the relative near-neighbour intensity at short cooling times. Note that while the near-neighbour intensity ratio changes little with burnup, the dependence of absolute Cherenkov light intensity on burnup is strong; high burnup implies high Cherenkov light intensity in both the fuel assembly emitting the radiation as well as in its neighbours.

### 2.3 Differences in the near-neighbour effect for BWR and PWR fuels

To investigate the differences in the near-neighbour effect for different fuel assembly configurations, the simulations in section 2.2 were complemented by simulations for a PWR case, where each PWR fuel was separated by a 5 mm steel wall, corresponding to closely stored fuel assemblies. In Figure 4, the ratios of NNR (see Eq. (1)) between BWR and PWR for the N1 and N2 positions are plotted, as a function of cooling time. The ratios are fairly flat at short cooling times, whereas for cooling times longer than 5 years, the near-neighbour intensity ratio, NNR, decreases more rapidly with cooling time for BWR as compared to PWR. This is likely due to a combination of

the changing gamma spectrum and thus the mean free path of the gamma rays with time, and the differences in distance between an active rod and the water in the neighbouring assembly for the two configurations. Accordingly, the near-neighbour effect depends on the fuel assembly configuration, and thus a compensation procedure may have to take the fuel type into account. Furthermore, one may note that NNR is higher for BWR fuel than for PWR fuel (the ratios between the fuel types is  $>1$ ), given that both assembly types are stored closely.

### 2.4 Effects of fuel assembly spacing

To investigate the dependence of the near-neighbour effect on the storage distance between fuel assemblies, the simulations in sections 2.2 and 2.3 were complemented with an additional more spacious storage geometry, which corresponds to the storage situation for BWR fuels at the Forsmark Nuclear Power plant, for comparison with the experimental results reported in [10]. In these simulations, each fuel assembly was surrounded by a 2.5 mm-walled square steel channel, similar to the storage rack found at Forsmark. For the PWR simulation, the same relative fuel distance, as compared to fuel size, was simulated as in the BWR case, and the same wall thickness (2.5 mm steel) was used. The results for each simulated configuration are presented in Table 2 for 1-year cooled 40 MWd/kgU burnup fuel.

Storage configuration	Fuel size [mm]	Wall thickness [mm]	Fuel assembly centre-to-centre distance, [mm]	N1 intensity ratio (NNR)	N2 intensity ratio (NNR)
BWR close	130	4.0	135	$2.84 \pm 0.03\%$	$0.39 \pm 0.02\%$
PWR close	215	5.0	220	$2.60 \pm 0.01\%$	$0.26 \pm 0.01\%$
BWR spacious	130	2.5 + 2.5	195	$1.43 \pm 0.02\%$	$0.54 \pm 0.02\%$
PWR spacious	215	2.5 + 2.5	322	$0.63 \pm 0.01\%$	$0.18 \pm 0.01\%$

**Table 2:** The near-neighbour intensity ratio (NNR in Eq. (1)) for two fuel types and two different fuel centre-to-centre distances. In the spacious simulations, each fuel was surrounded by a separate steel wall. In the simulations for the N2 intensities, the N1 positions were occupied. The uncertainties are due to statistics in the Monte-Carlo simulations, and are presented for the  $1\sigma$  level. The simulated fuel assemblies had a cooling time of 1 year and a burnup of 40 MWd/kgU.

As can be seen in Table 2, the near-neighbour intensity in N1 is smaller for the more spacious storage geometry. For position N2 in the BWR case, the intensity becomes higher. The reason is that the assemblies in N1 positions strongly attenuate radiation travelling between the Main and N2 position in the close storage configuration. In the more spacious storage configuration, the N1 fuels interfere less with the radiation from the Main assembly, leading to a net increase in the N2 intensity ratio, despite the increased distance between them. For the PWR case, the result in larger absolute distances in the spacious storage geometry lower the N2 intensity ratio. Had the simulated distance been smaller, it may have been possible to observe the same effects as for the BWR case.

### 3. Comparison of simulations with experimental results

In 2012, a series of measurements were conducted at the Forsmark nuclear power plant, where the near-neighbour effect was quantified for the N1, N2 and N3 fuel positions [10], when all other positions were vacant. This was done by; (i) moving one active fuel assembly (defined as “Main” in Figure 2) to an isolated location and measure it to record the  $I_{main}$  intensity of Eq. (1), and; (ii) place it relative to a fresh fuel assembly in the N1, N2 and N3 positions and measure the subsequent intensity increase in the fresh fuel assembly, corresponding to  $I_{neighbour}$  in Eq. (1). For details on these measurements, we refer to [9]. Here, the measured configurations have been simulated to provide an experimental benchmark of the simulation procedure, as further described below.

#### 3.1 Measured and simulated geometries

In the measurements, the active assembly was of one BWR 10x10 type, while the fresh fuel was a different BWR 10x10 design. The properties of the storage racks at the Forsmark plant are accounted for in Table 2, denoted “BWR spacious”. The irradiation histories of the fuel assemblies were made available to the authors, courtesy of the operator, Vattenfall.

In the simulations, the fuel irradiation histories were used to calculate the assemblies’ gamma emission spectra by means of the ORIGEN code [5]. Using these spectra, simulations were run for the Forsmark storage configuration. However, the fuels simulated were BWR 8x8, while the

irradiated fuels measured at Forsmark were all 10x10, including several part-length rods. The reason for not simulating the 10x10 fuel type was that information regarding the assembly manufacturer, and consequently the exact geometry data for the fuel types were unavailable for confidentiality reasons. However, the outer dimensions are similar for BWR 8x8 and 10x10 fuels, and both assembly types have a similar fuel to water ratio. Furthermore, differences in fuel pellet diameter results in different self-shielding by the rods, but an increase in absorption will lower both the Cherenkov light intensity in the assembly and in the neighbours, which partially compensates for the changes to the NNR. Consequently, the BWR 8x8 simulations may be considered to be representable also for 10x10 fuels in this context.

#### 3.2 Results

In Table 3, the simulated near-neighbour intensities are compared to the intensities measured at Forsmark [10]. The overall agreement is good, especially for the N1 position where the near-neighbour effect is the strongest. One may note that the N1 position is slightly underestimated, while the N2 and N3 positions are overestimated. The deviations may be explained by differences between the simulated and measured fuel assembly configurations, or by measurement uncertainties. Further investigations would be required to draw more solid conclusions on the deviations.

Another result of these simulations is that for fuel assemblies in this storage geometry, the N2 intensity is not much affected by the presence or absence of a fuel in the N1 positions. In the case of both N1 positions occupied, the simulated N2 NNR is  $0.41 \pm 0.01 \%$ , and with the N1 positions vacant it increases to  $0.43 \pm 0.01 \%$ .

### 4. Detection limits in presence of the near-neighbour effect

As mentioned in section 1.1, partial defect verification using the DCVD relies on the fact that a 50% substitution of rods with non-radioactive content will reduce the Cherenkov light intensity by at least 30%, which, accordingly, is taken as the limit for partial defect. Fuel assemblies where measured intensities are more than 30% lower than predicted are detected as being subject to partial defect, whereas other assemblies pass the inspection. This

Neighbour position	Measured neighbour intensity	Simulated neighbour intensity
N1	1.25%	$1.16 \pm 0.02\%$
N2	0.36%	$0.43 \pm 0.01\%$
N3	0.12%	$0.18 \pm 0.01\%$

**Table 3:** Comparison of the measured near-neighbour effect (data from [10]), to a simulated near-neighbour intensity for a similar configuration, which was obtained using a gamma spectrum calculated with ORIGEN, taking into account the operator-declared fuel irradiation history. Simulation uncertainties are due to the Monte-Carlo nature of the simulations. Uncertainties in the measurements were not provided in [10].

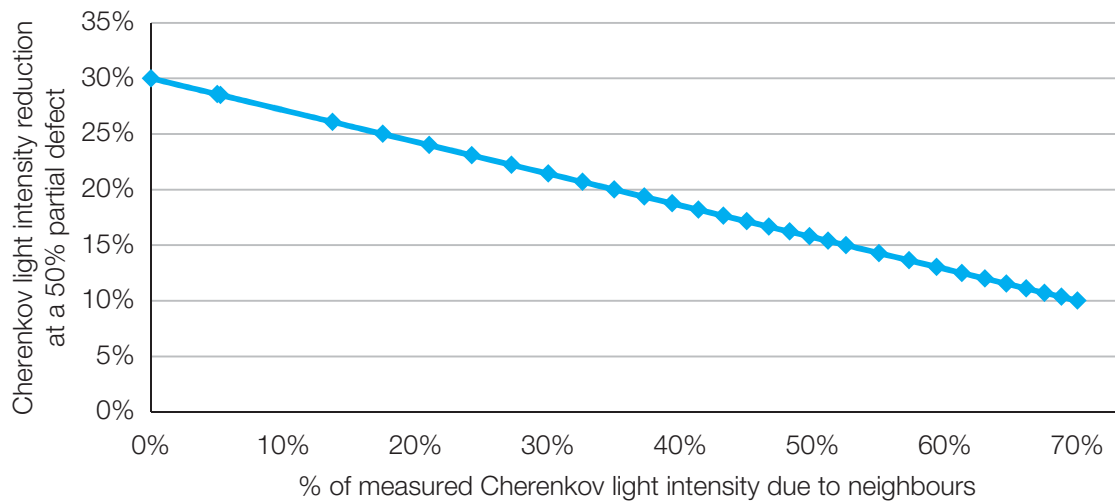


**Figure 5:** Calculated reduction of the 30% light intensity limit as a function of the near-neighbour intensity.

situation becomes slightly more complicated in presence of the near-neighbour effect, since the light being measured is partly caused by the fuel under study, and partly by the neighbouring fuels. As a consequence, the limit of 30% will be reduced when near-neighbour intensities influence the analysed data. This is shown in Figure 5, where the 30% intensity reduction is adjusted to also take into account the near-neighbour effect.

As a consequence of the data in Figure 5, the detection limit for partial defect at 30% lower intensity than expected would have to be lowered, unless the near-neighbour effect is corrected for. Lowering the detection limit would bring more stringent requirements on the accuracy of the models used for predicting the Cherenkov intensities as well as on the experimental precision that govern the accuracy of measured data in order to maintain the partial-defect detection capability. If the methods cannot meet these higher requirements, one must either allow a larger number of false alarms (using a lower threshold for partial defect according to Figure 5), or endanger the partial-defect detection rate (keeping the 30% intensity reduction threshold).

One situation where the near-neighbour effect would be particularly strong is when measuring a storage site with a population of neighbouring fuels with highly varying Cherenkov light intensities, due to largely varying burnups and cooling times. In such a situation, low-intensity fuel assemblies will be more strongly affected by the near-neighbour effect as compared to high-intensity ones. If the effect is not corrected for, the fuel intensity predictions will systematically underestimate the intensity of low-intensity fuels, while over-estimating the measured intensity of high-intensity fuels. Referring to Figure 5, considering a low-intensity assembly where as much as 50% of the intensity comes from neighbouring fuels, a diversion of 50% of its fuel rods may only cause a 15% decrease in measured intensity. It is doubtful that the current experimental and predictive methods may be further developed to offer the

precision required for confident detection in such extreme cases, unless the near-neighbour effect is included in the analysis.

In conclusion, to avoid changing the detection threshold while maintaining the partial-defect detection capability, methods for correcting for the near-neighbour effect should be considered. Such correction methods are further discussed below.

## 5. Methods for correcting for the near-neighbour effect

In this section, two methods for correcting for the near-neighbour effect are presented. The basics of both methods are that each measured intensity can be expressed as a sum of the intensity from the assembly under study,  $I_0$ , and the intensities from its nearest neighbours:

$$I_{measured} = I_0 + \sum_i (I_i \cdot \varepsilon_i) \quad (2)$$

Here,  $\varepsilon_i$  denotes the ratio of the intensity that neighbouring assembly  $i$  emits in the studied assembly to the intensity it emits in its own position, ( $I_i$ ). One may note that  $\varepsilon_i$  goes in the opposite direction compared to NNR defined in Eq. (1), but for symmetry reasons their values should be identical. The two methods presented below differ in how the  $\varepsilon_i$  are determined, where section 5.1 describes a method based on experimental data and section 5.2 describes a simulation-based method.

### 5.1 Least-squares fitting of experimental data

In [10], an experimental method to assess the near-neighbour effect was tested on a set of BWR fuel assemblies measured at Clab, under the conditions shown in Figure 2. The proposed method uses Eq. (2), limited to neighbours in relative positions N1 and N2 (referring to Figure 2). The method suggests collecting experimental intensities for the complete set of fuels in one storage rack and determining

the  $\epsilon_{N1}$  and  $\epsilon_{N2}$  factors by performing a least squares fit of Eq. (2) for the experimental data set, based on predicted intensities. These fitted  $\epsilon_{N1}$  and  $\epsilon_{N2}$  can then be used to predict the measured intensity of an assembly, given a prediction of the intensity of the assembly and its neighbours, or alternatively to subtract the intensity caused by the near-neighbour effect from the measurements.

Ref. [10] presents values of  $\epsilon_{N1}$  and  $\epsilon_{N2}$  obtained from fitting of the experimental data set. In this work, simulations of the storage conditions at Clab for the assemblies under study have been performed to provide an independent evaluation of the deduced values. A comparison of the simulated and the experimentally fitted intensities from [10] is shown in Table 4.

Neighbour	Simulated $\epsilon_i$	Fitted $\epsilon_i$
N1	1.82 ± 0.05%	16%
N2	0.17 ± 0.02%	9.5%

**Table 4:** Comparison of the simulated near-neighbour intensity for closely-stored BWR fuels (as shown in Figure 2) and the fitted values reported in [10].

Table 4 shows poor agreement between simulated and fitted values, and the simulations suggest that the fitted values overestimate the near-neighbour effect by almost an order of magnitude. Considering the relatively good agreement between simulations and measurements shown in Table 3, there is reason to suspect that the fitting procedure may not be adequate to accurately quantify the near-neighbour effect. Probable reasons for this deficit are that the fit is based upon a rather small set of fuels, and that the equation system may be ill-conditioned, making it sensitive to stochastic noise. One may assume better results if larger data sets are used or if constraints are introduced on the near-neighbour intensities, based on expected ratios.

## 5.2 Simulation-based corrections

As shown in section 3, simulations can provide relatively accurate estimates of the relative intensities from neighbouring fuel. However, since the near-neighbour simulations are time-consuming, a method is needed to take the near-neighbour effect into account in a quicker way, which can be used by inspectors in the field. Here, a solution is suggested, where the near-neighbour effect is parameterised as a function of fuel geometry, fuel centre-to-centre distance, and gamma-ray energy. The parameterisation would be based on large simulations done in advance, allowing for fast deployment for in-field inspections.

Based on the results presented here, primarily the N1 and N2 positions would need to be considered when assessing the near-neighbour intensity, and only rarely will the N3 position be significant. Given the irradiation history, or at

minimum the burnup and cooling time, of an assembly and all its neighbours, ORIGEN can be used to assess the gamma-ray energy spectrum of each fuel assembly. By binning the spectrum, it is possible to run simulations with initial gamma rays from each bin, to assess the near-neighbour intensity of gamma-rays of each energy. These simulations will have to be done for a large number of energy bins, for each fuel assembly configuration, and for several fuel centre-to-centre distances. The results will be the magnitude of the near-neighbour effect  $\epsilon_{i,j}$  for a fuel at neighbour position  $i$  and for gamma rays with energy in bin  $j$ . These simulations can be done in advance, and only have to be done once for each case.

To calculate the near-neighbour intensity at the event of measurement, the user selects the pre-calculated  $\epsilon_{i,j}$  values applicable for the fuel type and storage situation applicable to the measurement situation. These values are combined with the calculated, binned gamma-ray emission spectra of the neighbouring fuels, based on the operator declared fuel declarations. If the binned spectrum of a fuel is given by  $S_j$  for bin  $j$ , the intensity caused by one neighbour at position  $i$  ( $I_{neighbour,i}$ ) can then be calculated as:

$$I_{neighbour,i} = \sum_{j=1}^{\#bins} \epsilon_{i,j} \cdot S_j \quad (3)$$

The total near-neighbour intensity contribution in an assembly is then the sum of the intensity of all present neighbours, each calculated using Eq.3. This value can either be added to a predicted assembly intensity  $I_0$  to give a prediction of the measured intensity; alternatively it can be subtracted from the measurement to obtain an experimental value of assembly intensity  $I_0$  without neighbours.

## 6. Conclusions and outlook

Fuel assemblies in wet storage are often verified using the Digital Cherenkov Viewing Device, which enables inspection without requiring the fuel to be moved to an isolated measurement location. Since the fuel assemblies are stored closely, gamma rays from one assembly may enter a neighbouring assembly and create Cherenkov light, the so-called near neighbour effect. This paper describes how simulations can be used to estimate the magnitude of the Cherenkov light intensity that occurs in a neighbouring position due to the near-neighbour effect. The simulations have been validated using experimental data. The near-neighbour effect will be particularly influential in cases where long-cooled, low-burnup fuels containing relatively low activity levels are stored next to short-cooled, high-burnup fuels containing relatively high activity levels.

It has been shown that the partial-defect detection limits may need adjustment unless the near-neighbour effect is corrected for. Two possible methods for such corrections have been described; one method based on experimental



data and one simulation-based method. Building on the fact that simulations have proven capable reproducing experimentally recorded near-neighbour intensities, the latter method is recommended, and a methodology allowing for quick in-field use has been presented. The methodology is based on extensive, time-consuming simulations, which are done in advance to create parameterisations specific for storage configurations, assembly types and gamma-ray energies. These parameterisations may then be used for fast assessment during inspection.

While some experimental data is available regarding the near-neighbour effect, more is required to verify the simulations performed, and to assess the performance of the suggested method for predicting the near-neighbour effect. Knowing the accuracy of the near-neighbour prediction model will allow for higher limits to be set regarding what magnitude of near-neighbour effect can be tolerated in the measurements, which increases the partial-defect detection performance of the DCVD. Additional experimental data will also be useful for further refining the near-neighbour prediction model, which can further enhance the DCVD partial defect detection capabilities.

The studies presented in section 3 suggest that it may be possible to e.g. treat all BWR fuel assemblies as being identical with respect to the near-neighbour effect. Thus, it may be possible to simulate only a few selected fuel geometries of widely varying configuration, and use those simulations to assess the near-neighbour effect for all fuel types. This would greatly reduce the amount of simulations necessary to perform to parameterize the near-neighbour effect, but further studies are required to assess what uncertainties are introduced by this simplification.

## 7. Acknowledgements

This work was supported by the Swedish Radiation Safety Authority (SSM), under contract SSM2012-2750. The computations were performed on resources provided by SNIC through Uppsala Multidisciplinary Centre for Advanced Computational Science (UPPMAX) under project p2007011.

## 8. References

- [1] J. D. Chen et al., "Spent fuel verification using a digital cerenkov viewing device," 8:th International Conference on Facility Operations - Safeguards Interface, 2008.
- [2] J.D. Chen et al., "Partial defect detection in LWR spent fuel using a Digital Cerenkov Viewing," *Institute of Nuclear Materials Management 50th annual meeting*, 2009.
- [3] S. Rolandson, "Determination of Cherenkov light intensities from irradiated BWR fuel," IAEA task ID JNTA0704, SKI Report #: SE 1-94, 1994.
- [4] E. Branger, S. Grape, S. Jacobsson Svärd, P. Jansson and E. Andersson Sundén, "Comparison of prediction models for Cherenkov light emissions from nuclear fuel assemblies (accepted manuscript)," *Journal of Instrumentation*, 2017.
- [5] S. Bowman, L. Leal, O. Hermann and C. Parks, "ORIGEN-ARP, a fast and easy to use source term generation tool," *Journal of Nuclear Science and Technology*, vol. 37, pp. 575-579, 2000.
- [6] E. Branger, S. Grape, P. Jansson and S. Jacobsson Svärd, "Improving the prediction model for Cherenkov light generation by irradiated nuclear fuel assemblies in wet storage for enhanced partial-defect verification capability," *ESARDA Bulletin*, vol. 53, 2016.
- [7] Agostinelli, S, et al (the Geant4 collaboration), "Geant4 - a simulation toolkit," *Nuclear Inst. and Meth. in Physics Research Section A: Accelerators, Spectrometers, Detectors and Associated Equipment*, Volume 506, Issue 3, 1 July 2003, Pages 250-303.
- [8] S. Grape, S. Jacobsson Svärd and B. Lindberg, "Verifying nuclear fuel assemblies in wet storage on a partial defect level: A software simulation tool for evaluating the capabilities of the Digital Cherenkov Viewing Device," *Nuclear inst. and Meth. A*, Volume 698, 11 January 2013, Pages 66-71, ISSN 0168-9002, 10.1016/j.nima.2012.09.048.
- [9] S. Vacarro, S. Tobin, A. Favalli, B. Grogan, P. Jansson, H. Liljenfeldt, V. Mozin, J. Hu, P. Schwalbach, A. Sjöland, H. Trelue and D. Vo, "PWR and BWR spent fuel assembly gamma spectra measurements," *Nuclear Instruments and Methods in Physical Research Section A: Accelerators, Spectrometers, Detectors and Associated Equipment*, pp. 208-225, 2016.
- [10] D. Parcey, E. Sundkvist, J. Dahlberg, K. Axell, R. M Kosierb, B. Lindberg and S. Grape, "Determining the effect of adjacent spent fuel on Cherenkov light measurements," in *Institute of Nuclear Materials Management symposium*, 2012.